香港天文台
HONG KONG OBSERVATORY

Reprint 882

Development of Operational Rapid Update Non-hydrostatic NWP and Data Assimilation Systems in the Hong Kong Observatory

W.K. Wong

The Third International Workshop on Prevention and Mitigation of Meteorological Disasters in Southeast Asia, 1-4 March, 2010, Beppu, Japan

Development of Operational Rapid Update Non-hydrostatic NWP and Data Assimilation Systems in the Hong Kong Observatory

Wai-kin Wong

Hong Kong Observatory

134A, Nathan Road, Tsim Sha Tsui, Kowloon, Hong Kong, China

Abstract

The new operational numerical weather prediction (NWP) system of the Hong Kong Observatory, called the Atmospheric Integrated Rapid-cycle (AIR) forecast system, is discussed in this paper. AIR forecast system is based on the Non-hydrostatic Model (NHM) and its 3-dimensional variational analysis system developed by the Japan Meteorological Agency (JMA). It consists of two forecast domains with horizontal resolutions of 10 km and 2 km, which provides high resolution, rapidly updated analysis and numerical prediction from very-short-range (1-12 hours) to 3 days ahead. The performance of AIR forecast system will be illustrated through case studies including a tropical cyclone and a couple of rain cases. Outlines on the future research and development of AIR forecast system will also be given.

1. Introduction

A mesoscale NWP model system has been operated by the Hong Kong Observatory (HKO) using the Operational Regional Spectral Model (ORSM) since 1999. ORSM is formulated using the hydrostatic governing equations to provide numerical model guidance for short-term weather prediction up to 3 days ahead. The finest horizontal resolution is 20 km and the model run is updated every 3 hours. With the recent advances made in NWP modeling, HKO commenced the implementation and experimental trials of non-hydrostatic models few years ago, with a view to enhance the capability of quantitative precipitation forecast (QPF) and prediction of severe weather phenomena and mesoscale convective systems. In April 2004, HKO started to operate the JMA Non-hydrostatic Model (NHM) (Saito *et al.* 2006) in trial basis to provide very-short-range (1-12 hours) forecasts which are rapidly updated at every hour with high resolution (grid spacing at 5 km) covering an area of about 600 km x 600 km centred over Hong Kong. The initial and boundary conditions are obtained from the ORSM. In order to reduce the spin-up time of the model and improve the model QPF, the specific humidity fields of the cloud hydrometeors in NHM are initialized by the 3-dimensional cloud analysis output from the Local Analysis and Prediction System (LAPS) (Albers *et al.* 1996). Radar reflectivity, Doppler radial wind and geostationary satellite cloud data (visible albedo and infrared brightness temperature) are ingested into LAPS to generate the humidity fields of hydrometeors. Improvements in model QPF are obtained that facilitate the development of blending technique with nowcast QPF (Wong and Lai 2006). At the same time, forecasts from NHM are used to provide background data to LAPS for mesoscale real-time analysis with horizontal resolutions from few kilometres to few hundreds metres.

With experience gained on using JMA-NHM over the last few years, HKO will operate a new NWP system based on NHM, also called the Atmospheric Integrated Rapid cycle (AIR) forecast model system, by the rain season in 2010. AIR forecast model system has two forecast domains with horizontal resolution at 10 km and 2 km. With substantial increase in horizontal resolution, use of non-hydrostatic governing equations and more advance model physics, it is expected to bring enhancements in the capability to resolve mesoscale and local-scale weather phenomena, and their evolution from very-short-range to 3 days ahead.

In the paper, the design and experimental results of the AIR forecast system are described. In the next two sections, specifications of NHM and its data assimilation system will be presented. Performance of NHM in a couple of case studies on QPF, tropical cyclone movement and intensity, as well as the model verification on upper-level wind forecasts against aircraft data will be illustrated in Section 4. A short summary including aspects of future research and development of AIR system will be given in Section 5.

2. Description of NHM in AIR Forecast System

Figure 1 shows the coverage of the two NHM domains in AIR forecast model system. The outer domain, denoted by Meso-NHM, has the horizontal resolution at 10 km with 50 terrain-following vertical levels. Meso-NHM has an analysis-forecast cycle at 3 hours to provide forecast up to 72 hours ahead. It is targeted to simulate rainstorm, tropical cyclone track and intensity, and other mesoscale weather systems. The boundary condition of Meso-NHM is obtained from the forecasts of JMA Global Spectral Model (GSM) (JMA 2007) that are updated every 6 hours (initial time at 00, 06, 12 and 18 UTC) with horizontal resolution of forecast data at 0.5 degree in latitude and longitude. The sea-surface temperature (SST) is specified by the NCEP high resolution real-time daily SST analysis at 0.083 degree. The inner domain, called the RAPIDS-NHM, has horizontal resolution at 2 km with 60 vertical levels. Its boundary condition is based on the forecasts from Meso-NHM. The domain coverage is similar to the current trial operational 5-km NHM. RAPIDS-NHM provides forecasts up to 12 hours ahead and the model forecast is rapidly updated at every hour with a view to enhance the analysis and prediction of mesoscale and convective weather phenomena as well as to provide an improved model QPF to blend with the radar-based precipitation nowcast. More details on the specification of Meso-NHM and RAPIDS-NHM are given in the Table 1.

3. Data Assimilation System of NHM

The data assimilation of NHM in AIR forecast system is developed on the basis of JNoVA-3DVAR (**J**MA **No**n-hydrostatic model based **V**ariational data **A**ssimilation system). It is implemented as the hourly analysis system in JMA and the design is originated from the JNoVA-4DVAR (Honda *et al.* 2005) which is the operational data assimilation system for JMA Mesoscale Model (MSM) using NHM with horizontal resolution at 5 km (JMA 2007). Like the other variational data assimilation system, JNoVA-3DVAR computes the best linear unbiased estimate of the control variables representing the model states that minimize the following cost function:

$$J(\mathbf{x}) = \frac{1}{2}(\mathbf{x}-\mathbf{x_B})\mathbf{B}(\mathbf{x}-\mathbf{x_B})^T + \frac{1}{2}(\mathbf{y}-\mathbf{Hx})\mathbf{R}(\mathbf{y}-\mathbf{Hx})^T$$

where $\mathbf{x}$, $\mathbf{x_B}$ are respectively control variable vector and model background field. They include horizontal wind components (u,v), surface pressure (p_s), potential temperature (θ) and pseudo relative humidity representing the ratio of specific humidity of water vapour to its saturation value. $\mathbf{y}$ represents a vector containing observation data and $\mathbf{H}$ is the observation operator. $\mathbf{B}$ and $\mathbf{R}$ are respectively observation and background error covariance matrices

where **B** matrix is estimated based on the NMC method (Parrish and Derber 1992).

The observation data that can be assimilated in JNoVA-3DVAR include conventional observations from synoptic weather stations, radiosonde, buoy and ship reports, as well as data from automatic weather stations, wind profiler, aircraft measurements, atmospheric motion vector from geostationary satellites and retrieved ATOVS (Advanced TIROS Operational Vertical Sounder) temperature profile from NOAA polar-orbiting satellites. Total precipitable water vapour (TPWV) retrieved from microwave sounder (e.g. SSM/I) measurement and GPS (Global Positioning System) signals can also be assimilated to analyse the humidity contents. For the initialization of tropical cyclone, JNoVA-3DVAR includes a bogus scheme that will base on the forecaster's analysis on central pressure, maximum wind and radius of strong wind to construct vertical profiles of horizontal wind components around the tropical cyclones with asymmetric effects of storm structure taken into account. The wind profiles are then assimilated into JNoVA-3DVAR in a similar way as the other upper-air wind data but using different error characteristics. On the other hand, the current JNoVA-3DVAR cannot assimilate radar reflectivity directly for initialization of water vapour and humidity fields of cloud hydrometeors in NHM. Therefore, cloud data from geostationary satellites including the albedo and brightness temperature from visible and infrared channels respectively, and also the radar reflectivity are first ingested into LAPS to generate gridded TPWV analysis, and then assimilated into JNoVA-3DVAR as additional observation data.

4. Case Studies

In this section, discussions will be given to illustrate the performance of NHM in precipitation and tropical cyclone forecasts through a couple of case studies. Verification on the upper-level wind forecasts by NHM will also be discussed.

4.1 Rainstorm on 24 May 2009

On 24 May 2009, a broad area of low pressure affected the northern part of the South China Sea. Meanwhile, a ridge of high pressure was established over southeastern part of China that resulted in convergence of easterly and southerly airstreams and successive development of rainbands over the coastal areas (Fig. 2a - 2c). Figure 3a depicts the forecasts of sea-level pressure and hourly accumulated rainfall at 0400 UTC on 24 May 2009 from Meso-NHM initialized at 1800 UTC on 23 May. In 3DVAR analysis, automatic weather station data from Hong Kong and Guangdong, atmospheric motion vectors and ATOVS retrieved temperature profiles are assimilated in addition to the conventional

observations. Meso-NHM can successfully simulate the rainbands over the coastal water. It can be revealed from the forecasts of winds and relative humidity on 850 hPa and 700 hPa levels (Fig. 3b and 3c) that the development of rainbands is associated with the low-level jet of moist southeasterly winds (areas enclosed by the red isotach representing 20 knots and above). As the convection predicted by Meso-NHM is quite shallow, the precipitation forecast by the model is less than the actual rainfall from radar estimate. Fig. 3d shows the forecast at the same time by RAPIDS-NHM which is initialized by the 3-hour forecast from Meso-NHM including the specific humidity of the cloud hydrometeors. In general, the forecast rainbands from RAPIDS-NHM have more detailed structures due to increased in horizontal resolution, which are more consistent with rainbands shown on the radar imagery in terms of their size and orientation in northwest-southeast direction.

4.2 Rainstorm on 4 June 2009

Under the influence of an active trough of low-pressure, several heavy precipitation events occurred over the coastal areas of southern China. Figure 4a shows the forecast of sea-level pressure and 3-hour accumulated rainfall forecasts at 1700 UTC 3 June 2009 (0100 HKT on 4 June, with Hong Kong time = UTC + 8 hours). The initial time is 0900 UTC and boundary condition is obtained from GSM forecasts initialized at 00 UTC. Apart from observation data mentioned in 4.1 above, the total precipitable water analysis output from LAPS at horizontal resolution of 5 km are also assimilated in JNoVA-3DVAR. Due to coverage of radar data, only humidity field over the Pearl River Delta is adjusted. The forecast precipitation from Meso-NHM is mainly located over the coast which is consistent with the radar rainfall analysis (Fig. 4b). However, the intensity of rainfall is less than the actual, probably due to the coarser horizontal resolution that cannot resolve the convective process effectively. Figure 4c depicted the hourly precipitation and surface wind forecasts at 0030 HKT from RAPIDS-NHM. The initial time of the model is 1200 UTC 3 June 2009. It can be seen that the forecast rainfall amount is improved with the horizontal resolution increased to 2 km that can resolve the convective process more effectively. More significant rainfall is forecast over the northern part of the territory of HK with hourly precipitation amount exceeding 30 mm which is closer to the actual rainfall intensity. Discrepancy in the forecast location of rainbands still exists. For operational applications, phase correction technique (Wong et al. 2009) can be applied to relocate the rainband with a view to improve the skill of very-short-range rainfall forecasts by blending with nowcast QPF.

4.3 Typhoon Koppu (0915) – Effects of bogus in intensity change

Figure 5a shows the 3DVAR analysis of Meso-NHM on the surface wind and sea-level pressure of tropical cyclone Koppu (0915) at 1200 UTC 13 September 2009. Bogus wind

profiles are assimilated in the analysis. At that time, Koppu had just intensified into a tropical storm with maximum wind at about 35 knots. The analysed central pressure is 991 hPa that agrees with the forecaster's real-time analysis. Compared to the background field (Fig. 6a) as interpolated by the GSM forecasts, the intensity of Koppu is improved through the bogus data assimilation as the central pressure is deepened by about 9 hPa. The 24 hour and 48 hour of forecasts using the above 3DVAR analysis and first guess from GSM as initial conditions are given in Fig 5b-5c and 6b-6c respectively. The forecast tracks are shown in Figure 7a, indicating that tracks from the two experiments are quite similar, although the time of landfall from the two experiments both lag behind the actual track by about 12 hours. Nevertheless, the bogus data assimilation results in a better intensification trend of Koppu (Fig. 7b) as the winds on upper levels within the bogus region are strengthened. The maximum wind speed (MWS) near surface is increased by 22 knots in the 24 hour forecasts with bogus data assimilation while MSW is increased by only 5 knots in the other case.

4.4 Forecast performance of upper level winds

To examine the performance of Meso-NHM in short-term forecast of upper level winds, in particular for aviation forecast applications, numerical experiments are conducted for the period from May to July 2009 using GSM analysis and forecast runs at 00 UTC and 12 UTC as the initial and boundary conditions. Forecast upper level winds up to 30 hours are verified against AMDAR wind data measured by aircraft. Bilinear interpolation method is applied to obtain the model forecast wind at the observation location. Figures 8a and 8b are the time series on the percentage of root-mean-square errors in wind speed and wind direction under 5 m/s and 20 degree respectively. It can be seen that the performance of NHM is similar to the GSM and is better than both current operational 60 km and 20 km ORSM, even though no data assimilation is applied for NHM while ORSM runs are initialized by analyses using 3-dimensional optimal interpolation technique with observation data including aircraft data ingested. Figure 8c is the distribution of percentage wind vector error which is the magnitude of root-mean-square errors of the horizontal wind components and the percentage values are binned in the interval of 0.5 m/s on x-axis. It again shows NHM outperforms both 60 km and 20 km ORSM, with higher percentage of sample found for NHM with RMSE of wind vector less than 3 m/s. Study on the impact of JNoVA-3DVAR on the forecasts will be conducted in future to investigate possible gain in performance on the forecast of upper level wind.

5. Summary and Future Development

The design and implementation of the AIR forecast model system - the new operational NWP model and data assimilation systems in HKO, are discussed in this paper. With the increase in model resolution, use of non-hydrostatic governing equations and more advanced model physics, the AIR forecast system shows promising results to enhance the forecast capability of mesoscale and convective weather systems. The 3-dimensional variational assimilation system facilities the ingestion of more types of observation to improve the initial condition of NHM.

To further enhance the AIR forecast system in the next few years, research and development will be made on aspects like (a) the studies of optimal parameters in physical parameterization processes, (b) development of direct assimilation of satellite microwave radiance data and radar reflectivity in JNoVA-3DVAR, (c) ingestion of new types of remote sensing observation (e.g. moisture and temperature retrievals from ground-based radiometer) and (d) development NHM with sub-kilometre resolution to forecast local-scale or terrain-induced severe weather phenomena in Hong Kong. Applications of NHM for aviation forecast guidance and supporting collaborative research activities on NWP will also be explored.

Reference

Albers S., J. McGinley, D. Birkenheuer, and J. Smart 1996: The Local Analysis and Prediction System (LAPS): Analysis of clouds, precipitation, and temperature. *Weather and Forecasting*, **11**, 273-287.

Honda, Y., M. Nishijima, K. Koizumi, Y. Ohta, K. Tamiya, T. Kawabata and T. Tsuyuki, 2005: A pre-operational variational data assimilation system for a non-hydrostatic model at the Japan Meteorological Agency: Formulation and preliminary results. *Quart. J. Roy. Meteor. Soc.*, **131**, 3465−3475.

JMA, 2007: Outline of the Operational Numerical Weather Prediction at the Japan Meteorological Agency. *Appendix to WMO Technical Progress Report on the Global Data-processing and Forecasting System and Numerical Weather Prediction*, March 2007, 194 pp.

Parrish, D. and J.C Derber, 1992: The National Meteorological Center's spectral statistical interpolation analysis system. *Mon. Wea. Rev.*, **120**, 1747-1763.

Saito, K., T. Fujita, Y. Yamada, J. Ishida, Y. Kumagai, K. Aranami, S. Ohmori, R. Nagasawa, S. Kumagai, C. Muroi, T. Kato, H. Eito, and Y. Yamazaki, 2006: The Operational JMA Nonhydrostatic Mesoscale Model. *Mon. Wea. Rev.*, **134**, 1266-1298.

Wong, W.K. & E.S.T. Lai, 2006: RAPIDS – Operational Blending of Nowcast and NWP QPF. *2nd International Symposium on Quantitative Precipitation Forecasting and Hydrology*, Boulder, USA, 4-8 June 2006.

Wong, W.K., L.H.Y. Yeung, Y.C. Wang and M. Chen, 2009 : Towards the Blending of NWP with Nowcast — Operation Experience in B08FDP, *WMO Symposium on Nowcasting*, 30 Aug-4 Sep 2009, Whistler, B.C., Canada.

Table 1

Specification of Meso-NHM and RAPIDS-NHM in AIR Forecast System

	Meso-NHM	**RAPIDS-NHM**
Horizontal resolution	10 km	2 km
Horizontal grid	Arakawa-C	
Map projection	Mercator	
No. of grid points	401x321	241x241
Vertical coordinates	Terrain following height coordinates with Lorenz grid discretization	
No. of vertical levels	50	60
Time step	40 s	8 s
Initial time	00, 03, 06,…, 21 UTC	Every hour
Forecast range	72 hours	12 hours
Initial condition	First guess from JMA GSM 0.5 deg. data + JNoVA-3DVAR + LAPS cloud moisture analysis	First guess from Meso-NHM + JNoVA-3DVAR + LAPS cloud moisture analysis
Boundary condition	JMA GSM forecast data at 0.5 degree resolution in lat/lon	Meso-NHM forecasts
Nesting configuration	One-way nesting	
Topography	USGS GTOPO30 (30 second data smoothed to 1.5 times horizontal resolution) with modifications over HK areas based on USGS-SRTM (Shuttle Radar Topography Mission)	
Land-use characteristics	USGS Global Land Cover Characterization (GLCC) 30 second data and 24 land-use types with modification over HK areas	
Dynamics	Fully compressible non-hydrostatic governing equations solved by time-splitting horizontal-explicit-vertical-implicit (HEVI) scheme using 4-order centred finite differencing in flux form	
Cloud microphysics	3-ice bulk microphysics scheme (Ikawa and Saito 1991)	
Convective parameterization	Kain-Fritsch scheme (JMA version)	-
Surface process	Flux and bulk coeffcients: Beljaars and Holtslag (1991), Donelan et al. (2004), Belamari (2005) Roughness length: Beljaars (1995) and Fairall et al. (2003) Stomatal resistance and temporal change of wetness included 4-layer soil model to predict ground temperature and surface heat flux.	
Turbulence closure model and planetary boundary layer process	Mellor-Yamada-Nakanishi-Niino Level 3 (MYNN-3) (Nakanishi and Niino, 2004) with partial condensation scheme (PCS) and implicit vertical turbulent solver. Height of PBL calculated from virtual potential temperature profile.	
Atmospheric radiation	Long wave radiation process follows Kitagawa (2000) Short wave radiation process using Yabu and Kitagawa (2005) Prognostic surface temperature included; Cloud fraction determined from PCS.	

Figures

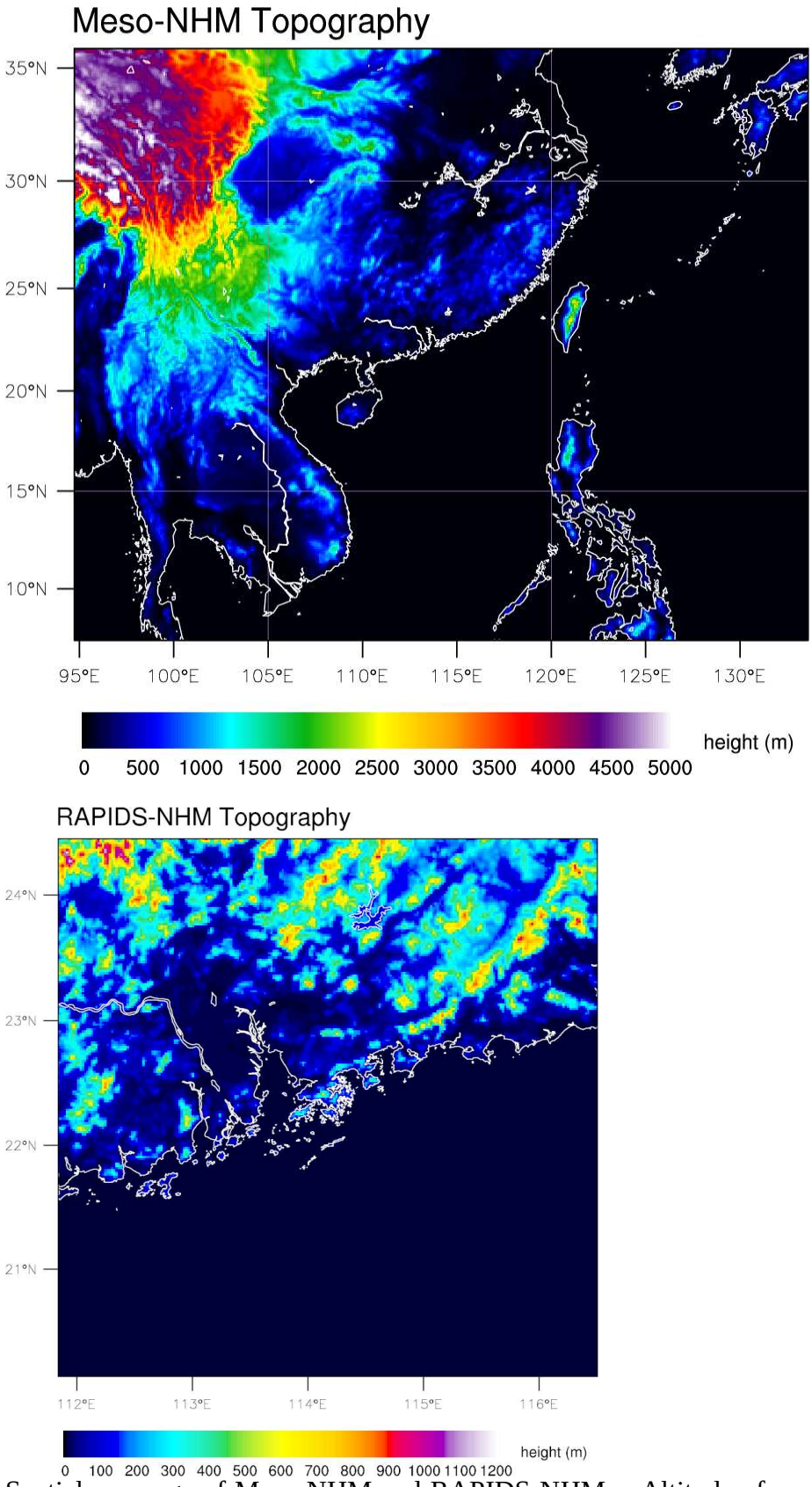

Fig. 1 Spatial coverage of Meso-NHM and RAPIDS-NHM. Altitude of model topography (in metre) is given in color shading.

(a)

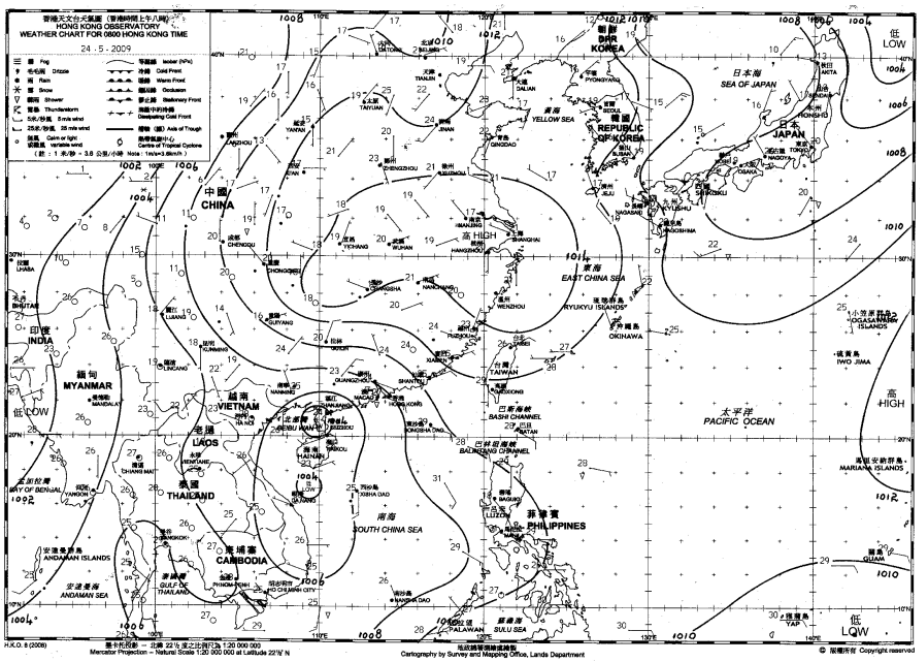

(b)

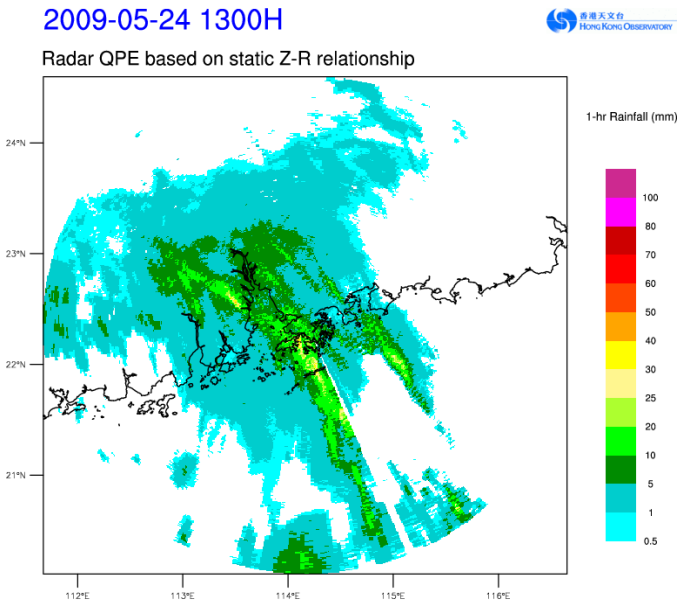

(c)

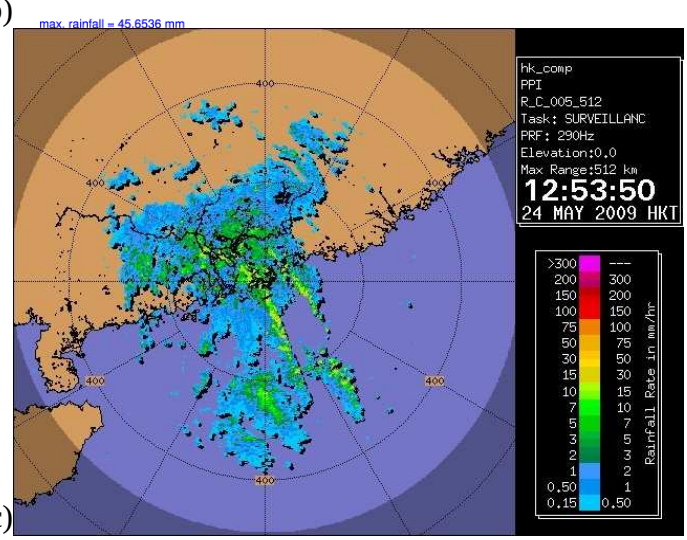

Fig. 2 (a) Synoptic analysis at 0000 UTC 24 May 2009 (0800 HKT); (b) Radar rainfall analysis of 1-hr accumulated rainfall (in mm) at 1300 HKT; (c) radar reflectivity imagery at 1253 HKT.

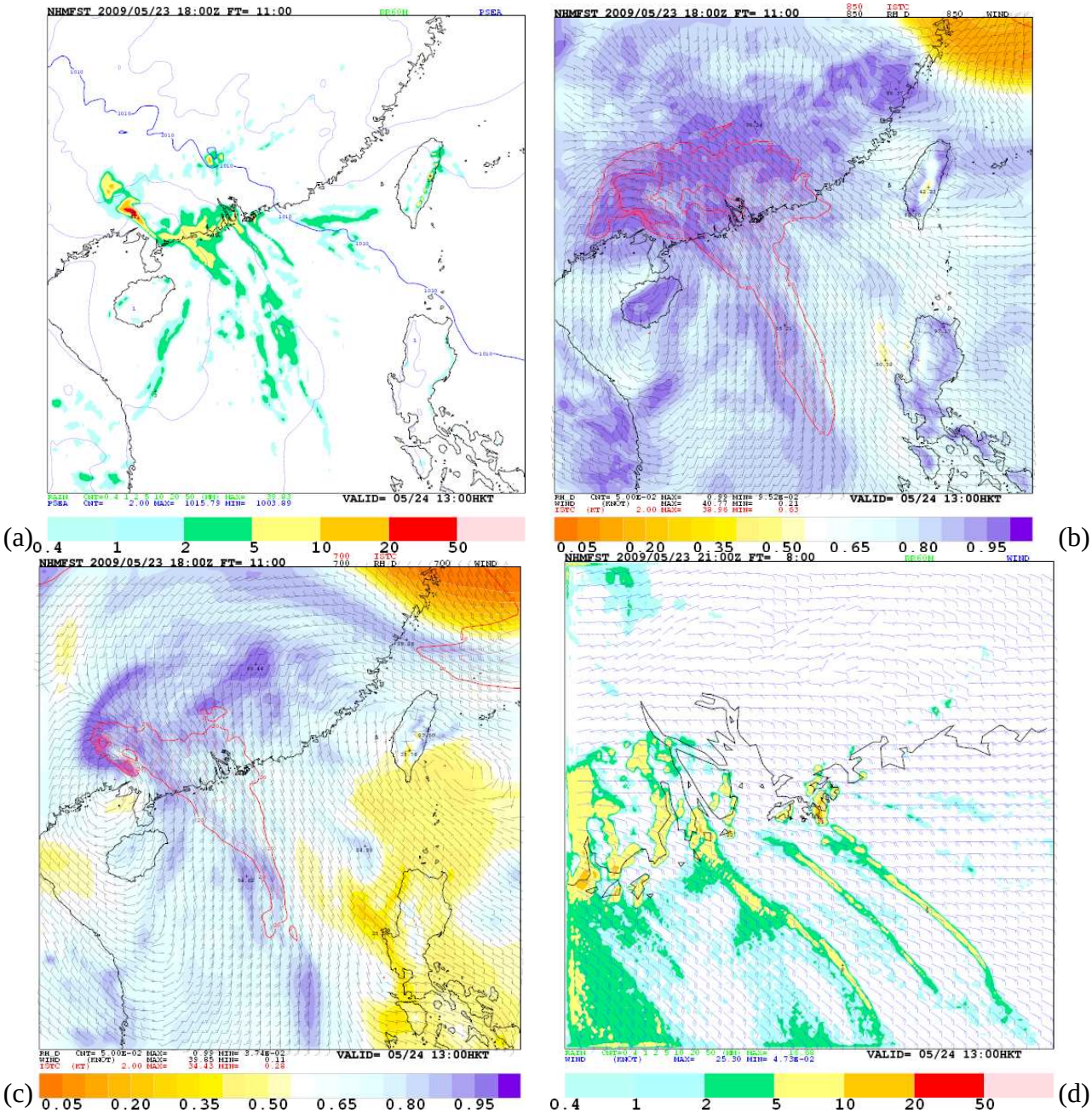

Fig. 3 (a) Forecast of sea-level pressure and 1-hour accumulated rainfall at 1200 HKT 24 May 2009 by Meso-NHM; Forecast of relative humidity (color) and winds on (b) 850 hPa and (c)700 hPa levels, areas enclosed by red contour representing wind speed exceeding 20 knots; (d) Forecast of 1-hour accumulated rainfall and surface wind at 1200 HKT by RAPIDS-NHM.

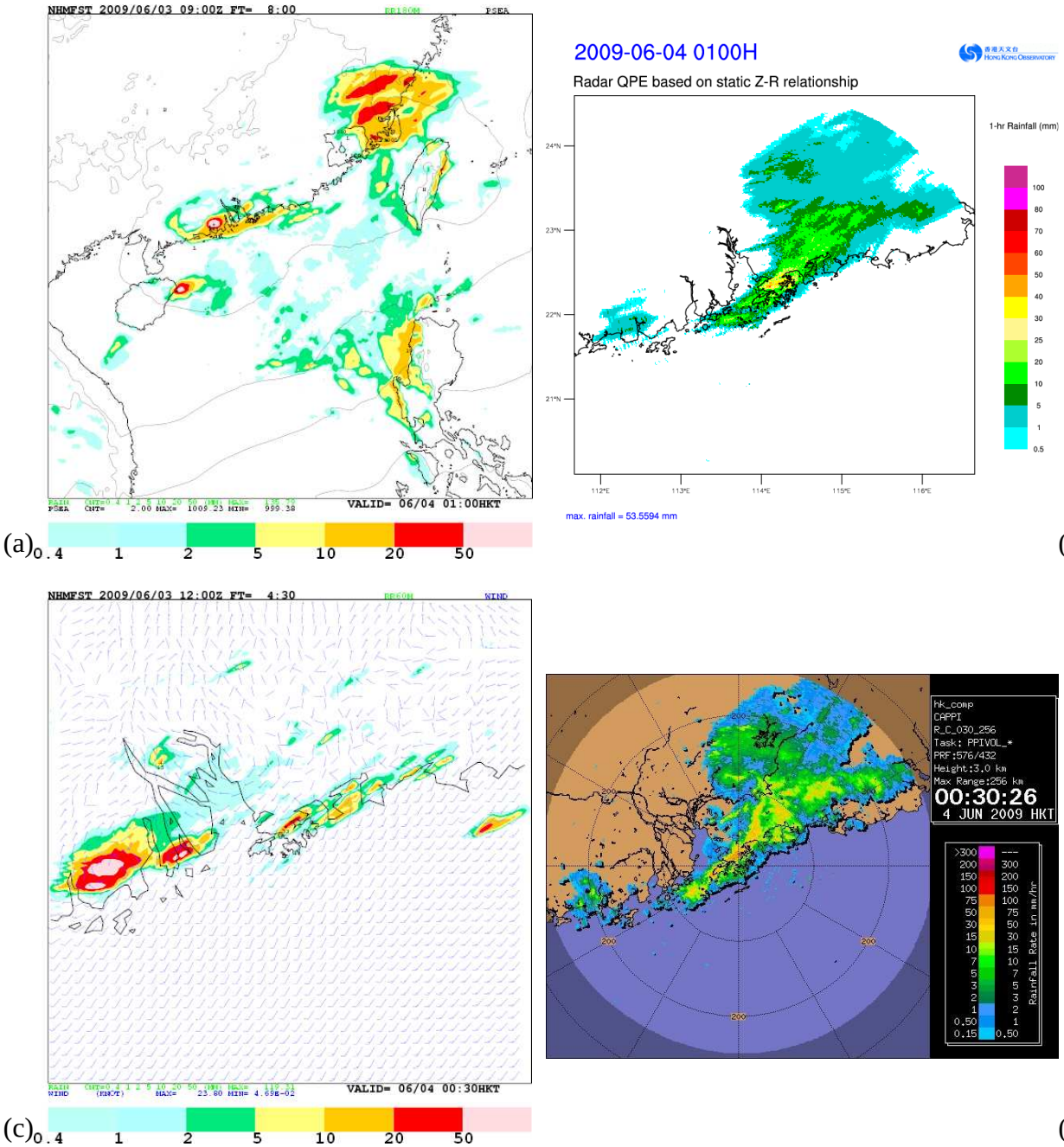

Fig. 4 (a) Forecasts of sea-level pressure (contour) and 3-hour accumulated rainfall (color) at 0100 HKT 4 June 2009 (1700 UTC 3 June 2009) by Meso-NHM; (b) radar-based quantitative precipitation estimates of 1-hour rainfall at 0100 HKT; (c) Forecasts of surface wind and 1-hour accumulated rainfall at 0030 HKT by RAPIDS-NHM; (d) radar CAPPI reflectivity at 3 km altitude at 0030 HKT.

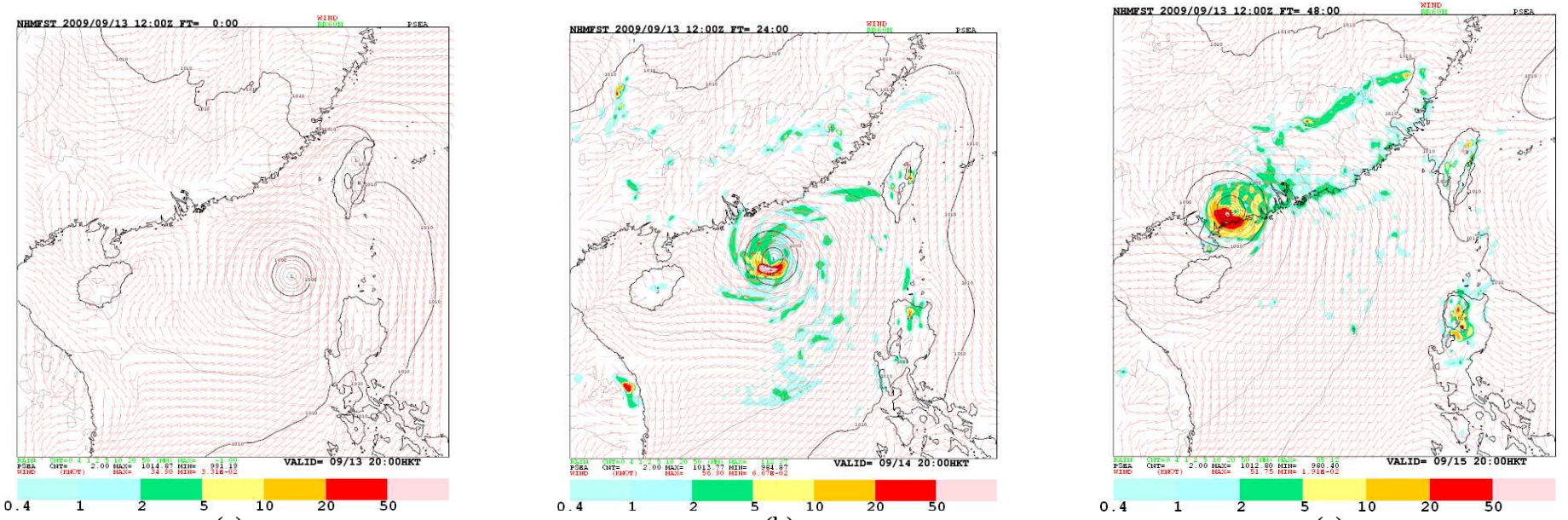

(a) (b) (c)

Fig. 5 (a) JNoVA-3DVAR analysis of surface wind, sea-level pressure at 12 UTC 13 September 2009 by Meso-NHM. (b)-(c) 24 hour and 48 hours forecast overlaid with 1-hour accumulated rainfall.

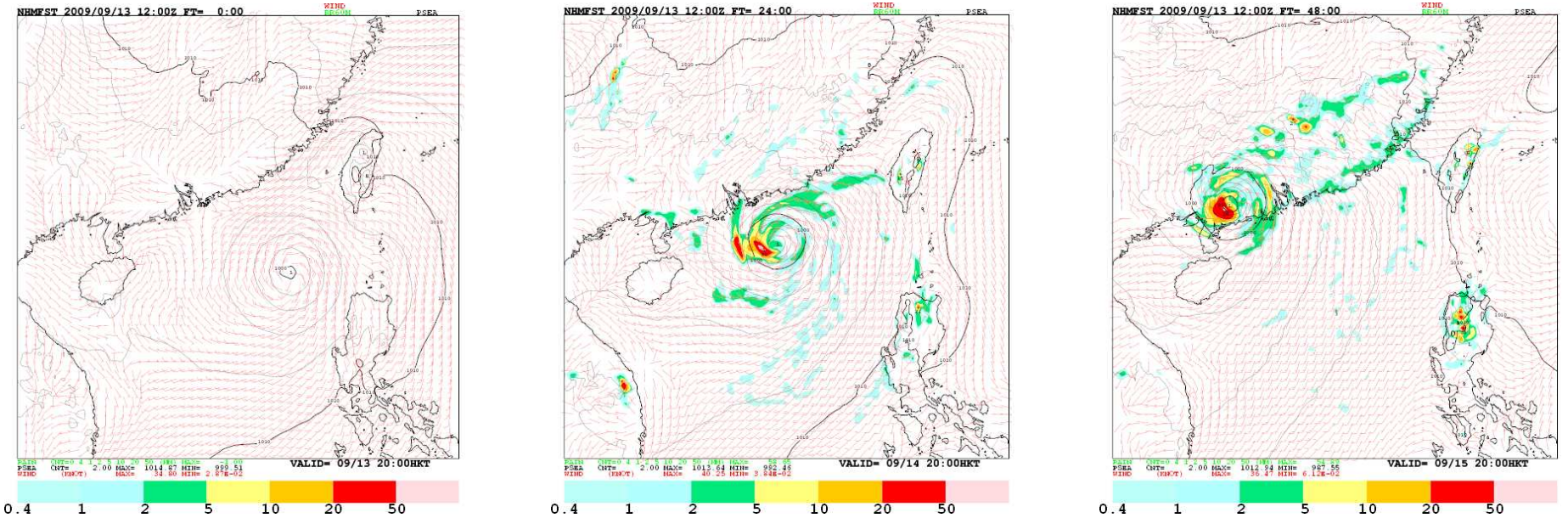

(a) (b) (c)

Fig. 6 Similar to Fig. 5 but the initial field is obtained without 3DVAR analysis.

(a)

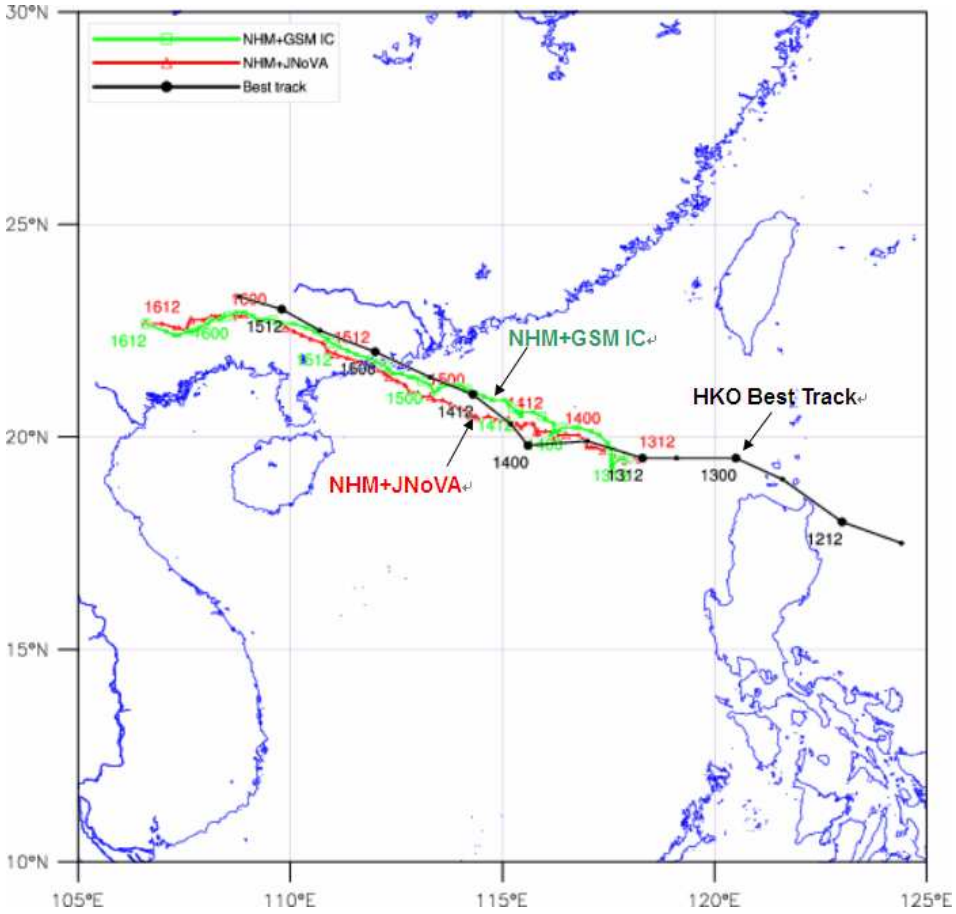

(b)

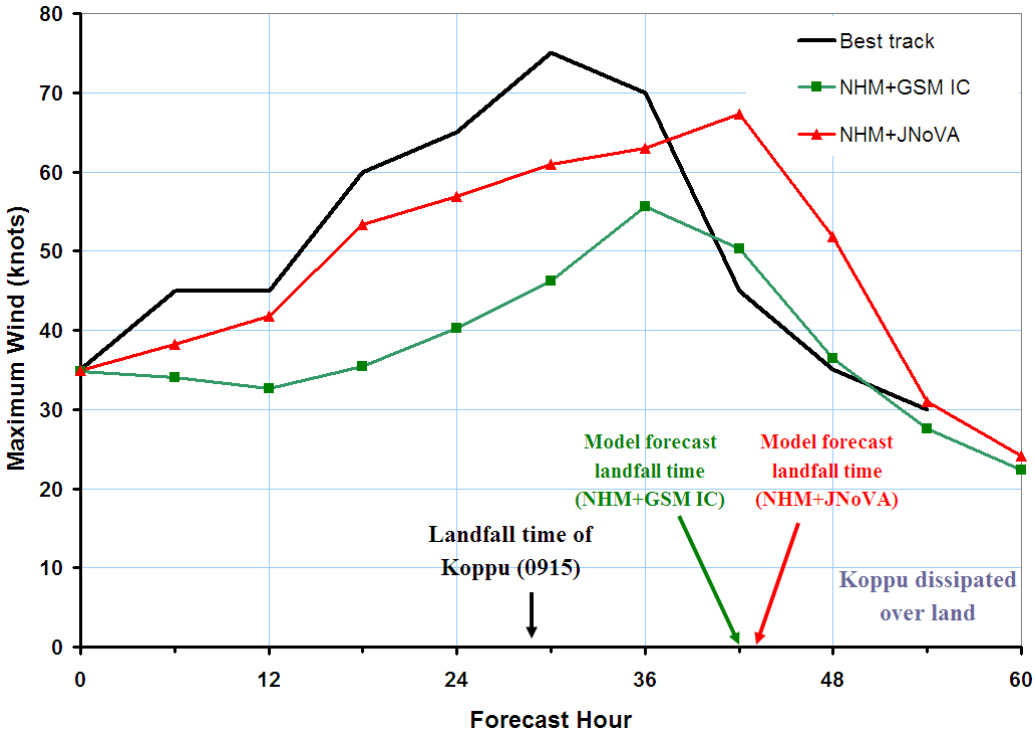

Fig. 7 (a) Forecast tracks of Koppu (0915) by Meso-NHM using JNoVA-3DVAR analysis (red line with triangle marks) and initial condition interopolated from GSM forecast (green line with square marks). HKO best track is shown in black line with dots indicating the 6-hourly positions; (b) Maximum wind near centre of Koppu by the two experiments. HKO best track data is shown in black line.

(a)

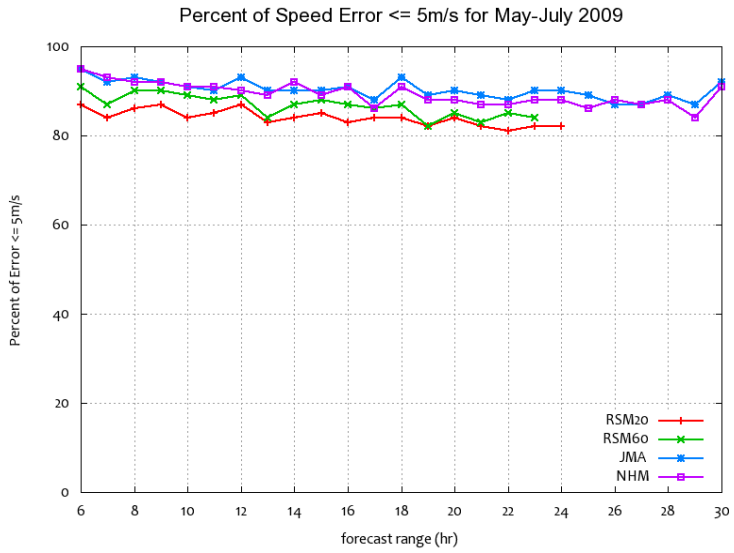

(b)

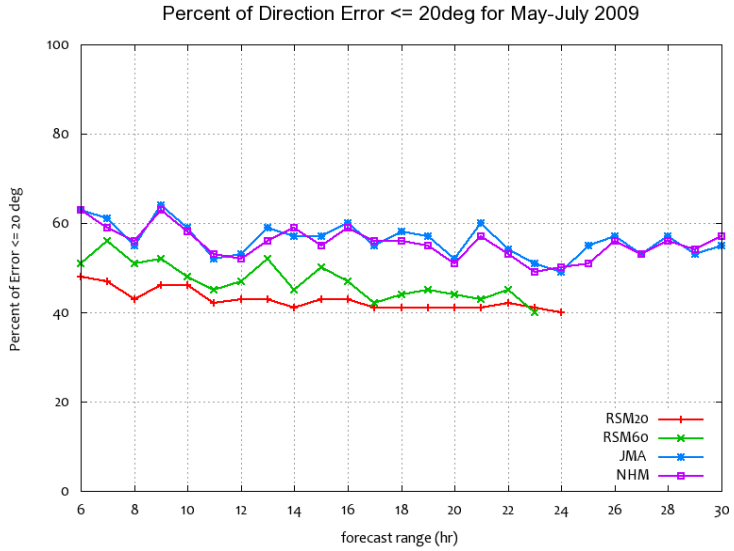

(c)

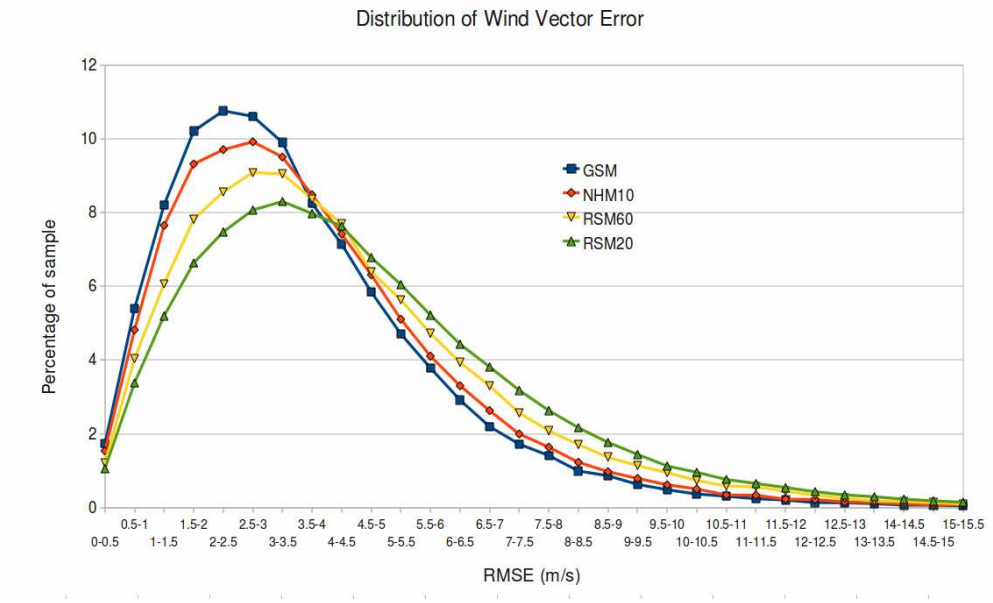

Fig. 8 (a) Time series of percentage of RMSE on wind speed forecasts within 5 m/s for NHM (purple line), GSM (blue line) and ORSM (red and green lines); Verification period from May to July 2009. (b) Similar to (a) but for percentage of RMSE on direction within 20 degree. (c) Distribution of RMSE of wind vector for GSM, NHM, and ORSM forecasts, with percentage of sample displayed in y-axis and RMSE binned in 0.5 m/s interval on x-axis.